Biomaterials Science

ROYAL SOCIETY OF CHEMISTRY

PAPER

View Article Online
View Journal | View Issue

Check for updates

Cite this: *Biomater. Sci.*, 2023, **11**, 4557

The effect of chondroitin sulfate concentration and matrix stiffness on chondrogenic differentiation of mesenchymal stem cells†

Chengchong Ai, [a,b] Ling Liu, [b,c] Kallista Wong,[b] Xuan Hao Tan[a,b] and James C. H. Goh*[a,b]

Chondroitin sulfate (CS), a glycosaminoglycan of native cartilage, has shown its potential in promoting chondrogenesis of mesenchymal stem cells (MSCs), whereas the effect of matrix stiffness in a CS-containing 3D environment on chondrogenesis is still poorly understood. Herein, this study aimed at assessing the effect of CS concentration and stiffness of CS-containing hydrogels on the chondrogenesis of MSCs. Hydrogels composed of 6% (w/v) gelatin methacryloyl (GelMA) and three concentrations, *i.e.*, 4%, 6%, or 10% (w/v), of methacrylated chondroitin sulfate (CSMA) were prepared. The hydrogels of each composition were prepared with two stiffness values (33.36 ± 8.25 kPa *vs.* 8.42 ± 2.83 kPa). Physical characterization showed similar microporous structures among the six groups, higher swelling ratios and faster degradation in the soft hydrogel groups. MSCs were encapsulated in the six groups of hydrogels and they underwent 28-day chondrogenic differentiation. The cell viability in each group on day 1 was similar and most cells exhibited a round shape without spreading. Afterwards, cellular protrusions in soft hydrogels remained filopodium-like from day 14 to day 28, while most protrusions were lamellipodium-like in stiff hydrogels on day 14 and then transformed into a spherical shape on day 28. The expression of chondrogenic markers analysed by real-time qPCR and immunohistochemical staining demonstrated that the optimal CS concentration for chondrogenesis was 6% (w/v) regardless of the stiffness of hydrogels. In addition, with the same CSMA concentration, the trend was observed that the stiff hydrogels supported superior chondrogenesis of MSCs compared to the soft hydrogel. To summarize, this study presents an advancement in the optimization of CSMA concentration and stiffness of hydrogels for chondrogenesis. In the CSMA/GelMA hydrogel, 6% (w/v) CSMA with an initial Young's modulus around 33 kPa was recommended for cartilage tissue engineering.

Received 2nd December 2022,
Accepted 24th April 2023

DOI: 10.1039/d2bm01980a

rsc.li/biomaterials-science

1. Introduction

As a thin layer of tissue which is responsible for load distribution, lubrication and protection of subchondral bones in the joints, the articular cartilage (AC) is prone to wear and tear or sports injury.[1,2] Cartilage defect is difficult to self-heal due to the avascular and aneural nature of cartilage tissue, and chronic and progressive degeneration of cartilage may cause disability in the long term.[3]

In the current clinical approaches to repair cartilage defects, such as microfracture, autologous chondrocyte implantation (ACI), or matrix-induced autologous chondrocyte implantation (MACI), bone marrow mesenchymal stem cell (MSCs) or autologous chondrocytes are used as the cell source for cartilage regeneration. However, the long-term effectiveness of these treatments is still controversial, and more efforts in developing novel techniques are necessary.[4–6] Cartilage tissue engineering is a promising approach to repairing cartilage defects. Among the various types of scaffolds for cartilage tissue engineering, hydrogels are commonly used as they closely mimic the highly hydrated natural 3D environment of tissues and can be tuned to guide cellular behavior toward the desired purpose.[7] Biochemical and biophysical cues in hydrogels play a crucial role in regulating cellular behaviours;[8] thus regulating these cues has the potential to engineer cartilage tissue.

Chondroitin sulfate (CS) is a natural polysaccharide in the ECM of native cartilage tissue. It has shown its potential as a

[a]*Integrative Sciences and Engineering Programme, NUS Graduate School, National University of Singapore, Singapore. E-mail: biegohj@nus.edu.sg; Fax: +65 68723069; Tel: +65 65165985*
[b]*Department of Biomedical Engineering, National University of Singapore, Singapore*
[c]*Institute for Health Innovation & Technology (iHealthtech), National University of Singapore, Singapore*

† Electronic supplementary information (ESI) available. See DOI: https://doi.org/10.1039/d2bm01980a

powerful biochemical cue to guide chondrogenesis of MSCs, displaying its advantages such as promoting chondrogenesis,[9,10] having an anti-inflammatory effect,[11–13] inhibiting hypertrophy,[14] and enhancing integration with native cartilage.[15,16] In the aspect of biophysical cues, it has been well-recognized that extracellular matrix stiffness could regulate stem cell fate.[17] However, the effect of the ECM's stiffness on MSCs' chondrogenesis in a 3D environment is still inconclusive. Regarding the effect of stiffness on the chondrogenesis of MSCs in a 3D environment containing CS, only one paper reported that in CS/poly-(ethylene glycol) dimethacrylate (PEG) hydrogels, the CS concentration of 5% (w/v) is optimal for chondrogenesis and a softer hydrogel with a Young's modulus of 7.5 kPa showed superior chondrogenesis of MSCs rather than the stiff hydrogel with a Young's modulus of 36 kPa.[18] One limitation of this CS/PEG hydrogel is the lack of cell binding motifs, which is a drawback in mimicking the native extracellular environment. CS exhibits weak cell affinity due to the lack of adhesive motifs,[19] but cell–matrix adhesion is important for enabling the cellular response to matrix stiffness.[20] Furthermore, it has been proved that cell binding sites could affect the chondrogenesis of MSCs in a hydrogel system.[21] Therefore, it is necessary to investigate the cellular response to stiffness during chondrogenesis in a CS-containing microenvironment more closely mimicking the native ECM.

To provide cell binding characteristics to the CS-containing hydrogel, gelatin methacrylol (GelMA) is chosen in this study since it contains cell adhesion domains and has been widely used in tissue engineering.[22] Methacrylated CS (CSMA) and GelMA are synthesized to fabricate the hydrogel system. Two variables, *i.e.*, stiffness and CSMA concentration, are included in the experimental setup as shown in Table 1, aimed to take advantage of both biochemical and biophysical cues in the hydrogel system for cartilage tissue engineering. In the stiff or soft groups, there are three subgroups classified by CSMA content and the experiment sample nomenclature is described in terms of (matrix stiffness) − (CSMA concentration). All six groups are named the stiff-low group (StL group), stiff-medium group (StM group), stiff-high group (StH group), soft-low group (SoL group), soft-medium group (SoM group), and soft-high group (SoH group). The objective of this study is two-fold: (1) investigating the influence of CSMA concentration on the chondrogenesis of MSCs and (2) assessing the chondrogenic differentiation capacity of MSCs in CSMA/GelMA hydrogels with different matrix stiffness, thus optimizing the combination of CSMA concentration and stiffness for cartilage tissue engineering.

Table 1 Experimental setup of this study

	CSMA content		
Stiffness	Low	Medium	High
Stiff hydrogel	StL group	StM group	StH group
Soft hydrogel	SoL group	SoM group	SoH group

2. Methods

2.1 Synthesis of CSMA and GelMA

CSMA was synthesized according to the published method.[23] CS was dissolved in distilled water at a concentration of 10% (w/v). 6.6 mL of glycidyl methacrylate (GMA) was added into the CS solution for 1 g of CS. The pH value of the mixed solution was adjusted to 3.5 using concentrated HCl and stirred at 60 °C protected from light. After reacting for 9 h, 12 h, and 48 h, the mixture was poured into ethanol. The precipitate was obtained after centrifuging and washing with ethanol at least 5 times. After drying in the oven at 60 °C, the solid CSMA was dissolved in distilled water and dialyzed with 10 kDa MWCO membrane for 2 days. After dialysis, pH of the CSMA solution was adjusted to 7.35–7.4 with 1 M sodium bicarbonate solution. The solution was filter sterilized using 0.22 μm syringe filters, freeze-dried, and stored at −20 °C.

GelMA was synthesized according to the published protocol.[22] Gelatin was dissolved in distilled water with a concentration of 10% (w/v). Methacrylic anhydride (MA) was added to the gelatin solution with two different weight ratios of MA to gelatin (0.1 g or 2 g of MA per 1 g of gelatin). The mixture was stirred for 3 hours at 50 °C and then centrifuged at 3500*g* for 3 min to remove the unreacted MA. The supernatant was diluted with two volumes of preheated distilled water and transferred into a dialysis tube with 10 kDa MWCO at 40 °C. To remove the cytotoxic MA and acid by-products, the dialysis lasted for 7 days. pH of the GelMA solution was adjusted to 7.35–7.4 with 1 M sodium bicarbonate solution. The solution was filter sterilized using 0.22 μm syringe filter, freeze-dried, and stored at −20 °C protected from light.

2.2 Nuclear magnetic resonance (NMR) measurements

The chemical structures of CSMA and GelMA were verified by proton NMR using D_2O as the solvent (^{1}H NMR, 500 MHz Bruker). For CSMA, the degree of functionalization (DoF) of CSMA was calculated as shown below:[24]

$$\text{DoF of CSMA} = \text{Area (new methyl groups after the reaction)}/\text{Area (methyl groups on the original CS)}.$$

The DoF of GelMA was defined as the percentage of lysine and hydroxylysine groups that were modified in GelMA.[25] First, the spectra were normalized to the aromatic signal which represents the concentration of gelatin. The ratio of the area under the lysine methylene signal of the GelMA spectra to that of the gelatin spectra represented the percentage of remaining unmodified lysine groups in the GelMA structure. The DoF of GelMA was calculated as shown below:[25]

$$\text{DoF} = 1 - \text{Area (lysine methylene of GelMA)}/\text{Area (lysine methylene of original gelatin)}.$$

2.3 Hydrogel preparation and mechanical characterization

Hydrogel precursor solution was prepared in PBS. Lithium phenyl-2,4,6-trimethylbenzoylphosphinate (LAP) was used as

the photoinitiator. 10% (w/v) CSMA hydrogels and 10% (w/v) GelMA hydrogels with two different concentrations of LAP, 0.05% and 0.1% (w/v), were used for mechanical testing. After mixing, the precursor solution was cast into polydimethylsiloxane (PDMS) mode with a diameter of 4 mm and thickness of 2 mm and UV-crosslinked (365 nm and 405 nm, 120 mW cm^{-2}) for 2 min. Unconfined compression tests were performed with an Instron machine fitted with a 10 N load cell at a rate of 1 mm min^{-1}. The stress–strain curve was plotted and the Young's modulus was calculated on the basis of the slope of the first 10% strain in the curve.

2.4 Compressive tests

To analyze the effect of LAP concentration and CSMA/GelMA ratio on Young's modulus of hydrogels, compressive tests were conducted on hydrogels of 10% (w/v) CSMA, 7% (w/v) CSMA + 3% (w/v) GelMA, 3% (w/v) CSMA + 7% (w/v) GelMA, and 10% (w/v) GelMA with LAP concentration of 0.02%, 0.03%, 0.05% (w/v).

To figure out the proper setup of each experimental group, 6% (w/v) of GelMA (high DoF or low DoF) was combined with 4% (w/v), 6% (w/v), and 10% (w/v) CSMA (high DoF or low DoF) for compressive tests. The LAP concentration was also adjusted for each CSMA/GelMA hydrogel complex.

The compressive test was also conducted on CSMA/GelMA hydrogels without cell encapsulation after UV crosslinking, after swelling equilibrium, and cell-laden hydrogels after culture in chondrogenic medium for 28 days.

2.5 Swelling behaviour and degradation of CSMA/GelMA hydrogels

The swelling properties of CSMA/GelMA hydrogels were measured as follows. Different hydrogel complexes were prepared and weighed after UV-crosslinking followed by incubation in PBS at 37 °C for 4 h, 24 h, 48 h, and 72 h. The hydrogel samples were blotted with KimWipe paper to remove the liquid on the surface before weighing on the balance. In addition, after UV-crosslinking, the hydrogels were freeze-dried and weighed as W_d. Subsequently, they were immersed in PBS for 24 h at 37 °C and weighed as W_s. The swelling ratio was calculated as Swelling ratio = $(W_s - W_d)/W_d \times 100\%$.

To investigate the degradation of CSMA/GelMA hydrogels, the hydrogel samples were incubated in PBS at 37 °C with PBS changed every 3 days. After washing with distilled water and lyophilization, the dry weight of each hydrogel was measured on day 1, day 3, day 5, day 15, and day 30. The percentage of residual weight was normalized to the dry weight on day 0. Four hydrogel samples were used for each group.

2.6 Morphology observation

The hydrogel samples of each group were prepared and immersed in PBS for 4 h for equilibrium. After being frozen and freeze-dried, the samples were immersed in liquid nitrogen and cut to expose the inner structure. The samples were observed using a scanning electron microscope (SEM, FEI Quanta 650 FEG) after gold coating.

2.7 Cell encapsulation and culture

Porcine bone marrow mesenchymal stem cells (MSCs) were isolated by bone marrow aspiration and cultured in an expansion medium composed of Dulbecco's Modified Eagle's Medium (DMEM low glucose, GlutaMax™ supplement, Thermo Fisher Scientific) with 10% (v/v) fetal bovine serum (FBS, Thermo Fisher Scientific) and 1% (v/v) penicillin/streptomycin solution (Thermo Fisher Scientific). Passage 3 MSCs were suspended in the precursor solution of each group at a density of 10 million per mL. Then 15 μL of each precursor solution was transferred into PDMS modes with a diameter of 4 mm and thickness of 2 mm, followed by UV-crosslinking (365 nm and 405 nm, 120 mW cm^{-2}) for 2 min. Meanwhile, 1.5×10^4 MSCs which contained the same amount of MSCs in each hydrogel sample were centrifuged at 1500 rpm for 5 min to form pellets. The cell–hydrogel constructs and pellets were cultured for 4 weeks in a chondrogenic differentiation medium (StemPro™ Chondrogenesis Differentiation Kit, Thermo Fisher Scientific).

2.8 Cell viability and metabolism

The cell metabolic rate of each group was measured using AlamarBlue assay (Bio-Rad) on days 1, 7, 14, 21, and 28. Chondrogenic medium and AlamarBlue reagent were mixed in a volume ratio of 10 : 1. The hydrogels or pellets were incubated in a medium containing AlamarBlue reagent for 4 hours, after which the medium was transferred into a transparent 96-well plate to measure the absorbance at 570 nm and 600 nm. The cell metabolic rate of each hydrogel was calculated according to the instruction of the manufacturer.

On day 1, live and dead cells were visualized using calcein AM and ethidium homodimer-1 (LIVE/DEAD™ Viability/Cytotoxicity Kit, Thermo Fisher Scientific). Hydrogels encapsulated with cells were incubated in DMEM solution of 10 μM calcein AM and 5 μM ethidium homodimer-1 for 15 min at 37 °C and then washed with PBS. Images were captured with a Zeiss LSM710 confocal microscope.

2.9 Cell morphology

The F-actin cytoskeleton was visualized by phalloidin staining. After being cultured for 14 days and 28 days, the hydrogel encapsulated with cells was fixed with 4% (w/v) formaldehyde overnight. After washing twice in PBS, the fixed hydrogels were permeabilized with 0.1% Triton X-100 in PBS for 10 min and then incubated in 1% bovine serum albumin (BSA) containing 3.3 μM Texas Red™-X phalloidin (Thermo Fisher Scientific) overnight. DAPI staining (NucBlue™ Fixed Cell ReadyProbes™ Reagent, Thermo Fisher Scientific) was applied for 15 min. Images were captured with a Zeiss LSM710 confocal microscope and processed with the Zen Black and Imaris software.

2.10 Gene expression analysis

Quantitative RT-PCR was performed to analyse chondrogenic and related gene expression. After culturing for 14 and 28 days, hydrogels or pellets were transferred into microcentrifuge

Table 2 Primer sequences for RT-PCR analysis

Genes	Entry name	Forward	Reverse	Product length
GAPDH	XR_002343817.1	GTA TGA TTC CAC CCA CGG CA	CAC CCC ATT TGA TGT TGG CG	122
SOX9	NM_213843.2	GCAAACTCTGGAGACTGCTG	TCTTCACCGACTTTCTCCGC	132
Col II	XM_021092611.1	GATGGCTGCACGAAACACAC	GACAGGCCCTATGTCCACAC	147
ACAN	NM_001164652.1	CAACCACGGCAGACTTTGAC	TCACACAGGTCCCCTTGGTA	121
Col X a1	NM_001005153.1	AGCTCCCAACATCCAGAATCC	AACTGTGCCTTGGTGTTGGA	159
COL1A1	XM_021067153.1	CGACGGATTCCAGTTCGAGT	CCGGATCTCGATCTCGTTGG	205
COMP	XM_003123527.3	AGATAACGCTGGGTGCAGAC	GTCACACTCCATCACCGTGT	143

tubes and pulverized using a microhomogenizer. Total RNA was extracted with an RNeasy Mini Kit (QIAGEN) following the manufacturer's protocol. The final eluted RNA was reverse transcribed to cDNA using the iScript™ cDNA synthesis kit (Bio-Rad). Quantitative RT-PCR was conducted in the QuantStudio 5 system (Thermo Fisher Scientific) using iTaq™ Universal SYBR® Green Supermix (Bio-Rad). The analyzed genes included SOX9, collagen II (Col II), collagen I (Col I), collagen X (Col X), ACAN, COMP, and GAPDH. The primer sequences of the genes are listed in Table 2. GAPDH was used as the housekeeping gene, and the relative expression level for each gene was calculated by the $^{\Delta\Delta}Ct$ method compared to undifferentiated MSCs.

2.11 Histology and immunohistochemistry

After culturing for 14 days and 28 days, hydrogels encapsulated with cells and chondrogenic pellets were fixed with 4% (w/v) formaldehyde overnight and then washed with PBS. Subsequently, the hydrogel samples were immersed in optimal cutting temperature compound (OCT compound, VWR) and PBS mixture with a volume ratio of 1 : 1 at 4 °C overnight. The samples were then fixed in OCT at −20 °C and sectioned at a thickness of 10 μm using a cryostat (Leica CM3050S). Chondrogenic pellets were dehydrated and embedded in paraffin and sliced using a microtome at a thickness of 5 μm. Alcian blue staining was applied first.

Immunohistochemistry (IHC) staining was conducted using a HRP/DAB detection kit (Ab64264, Abcam). Primary antibodies as the target for Col II antibodies (dilution ratio 1 : 100, ab 34712, Abcam) and SOX9 (dilution ratio 1 : 100, ab 185966, Abcam) were used. Enzymatic antigen retrieval with pepsin and heat-mediated antigen retrieval with sodium citrate buffer were performed before Col II antibody and SOX9 antibody incubation respectively. After primary antibody incubation at 4 °C overnight, the slides were treated with biotinylated goat anti-polyvalent, streptavidin peroxidase, and DAB reagent as per the manufacturer's instruction. Images were captured with a microscope (Olympus IX71). Hydrogel samples without cell encapsulation were also processed as a control. Image J was used to quantify the integrated optical density (IOD) of positive staining for each section.

2.12 Statistical analysis

All quantitative results are presented as mean ± standard deviation. Statistical significance was determined by analysis of one-way or two-way ANOVA followed by Tukey's *post hoc* test with the Prism software (Prism, GraphPad Software Inc.) for three or more groups. The comparison between two groups was conducted by Student's *t*-test. *P* value less than 0.05 was considered statistically significant.

3. Results

3.1 ^{1}H NMR spectra of CSMA and GelMA

The synthesis of CSMA is illustrated in Fig. 1A. On the ^{1}H NMR spectra of CSMA, two peaks at 6.0–6.2 and 5.6–5.8 ppm are attributed to the two protons attached to the double bond (C═CH_2); the peak at 1.9–2.0 ppm is ascribed to the methyl group adjacent to the double bond (CH_3–C═CH_2). The presence of these peaks in CSMA confirmed the methacrylation reaction. The peak at 2.0–2.2 ppm corresponded to the methyl group on the original CS. The DoF of CSMA was calculated from the ratio of the area under 1.9–2.0 ppm to the area under 2.0–2.2 ppm. The DoFs of CSMA after reaction of 9 h, 12 h, and 48 h were 0.243 ± 0.025, 0.333 ± 0.015, and 0.437 ± 0.045 respectively. The CSMA yielded from 9-hour and 48-hour reaction was named low-DoF CSMA (L-CSMA) and high-DoF CSMA (H-CSMA) respectively.

The synthesis of GelMA is shown in Fig. 1B. The reactive functional groups, which are located on the side groups of amino acid residues, included hydroxyl groups from serine, threonine, hydroxyproline, and hydroxylysine residues and amino groups from lysine and hydroxylysine residues.[26] Compared to unmodified gelatin, new signals were observed in the spectra of GelMA at 5.3–5.8 ppm and 1.9–2.0 ppm, which are attributed to the double bond (C═CH_2) and the methyl group adjacent to the double bond (CH_3–C═CH_2). The signal for 2.9–3.06 ppm corresponded to the protons of methylene of the lysine signal. The decrease of this signal confirmed that lysine amino acid had reacted with MA. The proton signal of the aromatic amino acid (7.2–7.5 ppm) in gelatin remained unchanged so that it was used to normalize the intensity of other protons in different samples. A higher MA amount in the synthetic reaction resulted in a higher DoF.[26] The DoF of GelMA after reaction with different weight ratios of MA were 0.508 ± 0.073 and 0.969 ± 0.017 and named low-DoF GelMA (L-GelMA) and high-DoF GelMA (H-GelMA) respectively.

3.2 Young's modulus of hydrogels without cell encapsulation

The stiffness of H-GelMA, L-GelMA, H-CSMA, and L-CSMA was determined by compressive tests. As expected, higher DoF and

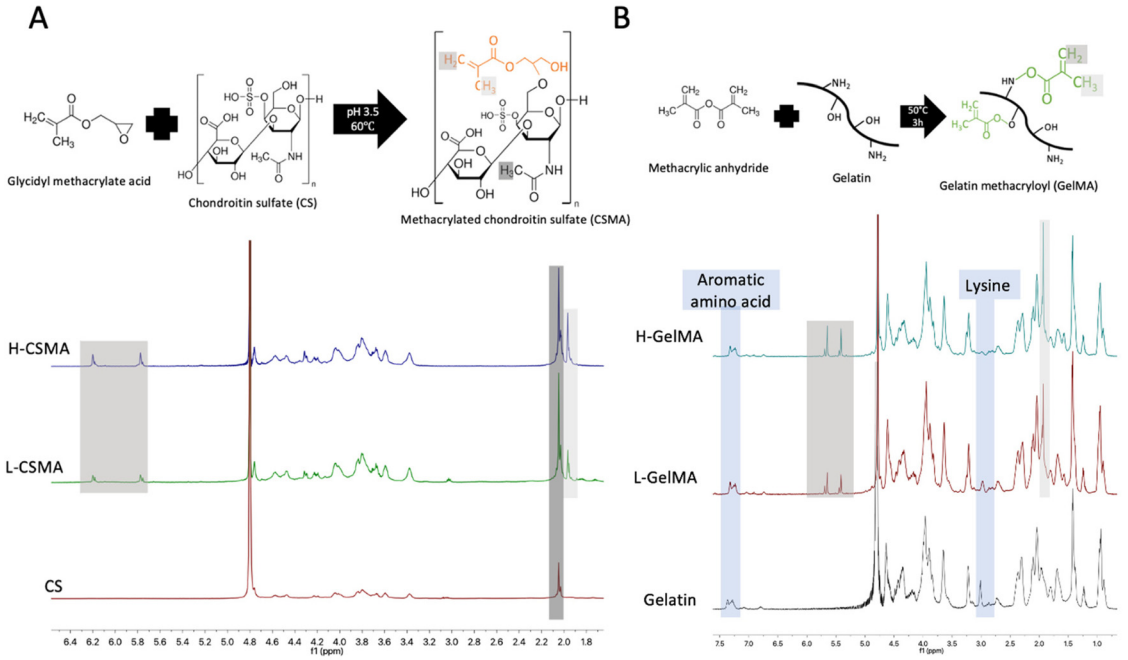

Fig. 1 Synthesis and ^{1}H NMR spectra of CSMA (A) and GelMA (B). The white and grey shadows marked the peak ascribed to the methyl group adjacent to the double bond and the double bond; the black shadow marked the methyl group on the original CS.

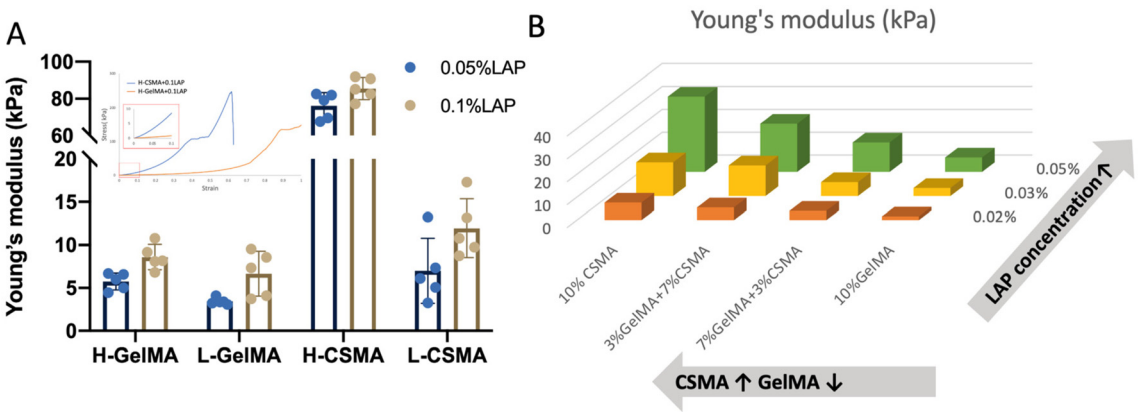

Fig. 2 Young's modulus of CSMA and GelMA (A); the effect of LAP concentration and CSMA/GelMA ratio on Young's modulus of CSMA/GelMA composite hydrogels (B).

increased LAP concentration resulted in hydrogels with increased Young's modulus (Fig. 2A). As shown in the stress–strain curves, H-CSMA had broken suddenly and H-GelMA was compressed until 100% strain, indicating that H-CSMA was much stiffer than H-GelMA.

Further on, CSMA (DoF = 0.333 ± 0.015) was mixed with H-GelMA in different combinations for compressive tests. It was found that even though the GelMA concentration had decreased, increasing the CSMA concentration resulted in a higher modulus (Fig. 2B). By adjusting the LAP concentration from 0.02% to 0.05%, the modulus of 10% CSMA increased from 6.71 ± 1.86 kPa to 32.94 ± 4.80 kPa, while 10% GelMA changed from 1.61 ± 0.42 kPa to 6.32 ± 1.36 kPa. All these findings indicated that CSMA played a dominant role in determining the modulus of CSMA/GelMA composite hydrogels.

3.3 Experimental setup and swelling ratio

To investigate the effect of CSMA content on the chondrogenesis of MSCs, three different CSMA concentrations (w/v), 4%, 6%, and 10%, were mixed with 6% GelMA. Because higher CSMA content would lead to a higher modulus, a lower concentration of LAP and L-GelMA were used as a trade-off in the groups containing a high concentration of CSMA. After modifying the LAP concentration for each combination of CSMA/

GelMA hydrogels as shown in Fig. 3A, finally the stiff groups and soft groups showed an average modulus of 33.36 ± 8.25 kPa and 8.42 ± 2.83 kPa, respectively. A heterogeneous porous structure was observed in each group (Fig. 3B). Unexpectedly, no relation between the pore size and CSMA concentration or stiffness was observed, which could be due to the varied LAP concentration and DOF of polymer in different groups.

To investigate the swelling behaviour of each group, the hydrogels were immersed in PBS after UV-crosslinking and the weight change was recorded (Fig. 3C–H). In all six groups, hydrogels reached swelling equilibrium within 4 hours as there was no difference in the weight between 4 hours and 24 hours in each group. The increase of weight after 24 hours was observed in the StL and StM groups, which could be due to the hydrolytic degradation lowering the crosslinking density of the hydrogel, allowing more water to diffuse into the hydrogels. In soft groups, especially the SoL group and SoM group, the hydrogels were too soft to be transferred after 48 h, indicating the fast degradation and dissolving of soft hydrogels. This was consistent with the observation from the degradation study. As shown in Fig. 3I, the soft groups degraded faster than the stiff groups. On day 15, two out of four samples in

A

Group name	Composition (w/v)				
	H-CSMA	L-CSMA	H-GelMA	L-GelMA	LAP
StL group	4%	/	6%	/	0.2%
StM group	6%	/	6%	/	0.1%
StH group	10%	/	/	6%	0.02%
SoL group	/	4%	6%	/	0.08%
SoM group	/	6%	6%	/	0.04%
SoH group	/	10%	/	6%	0.04%

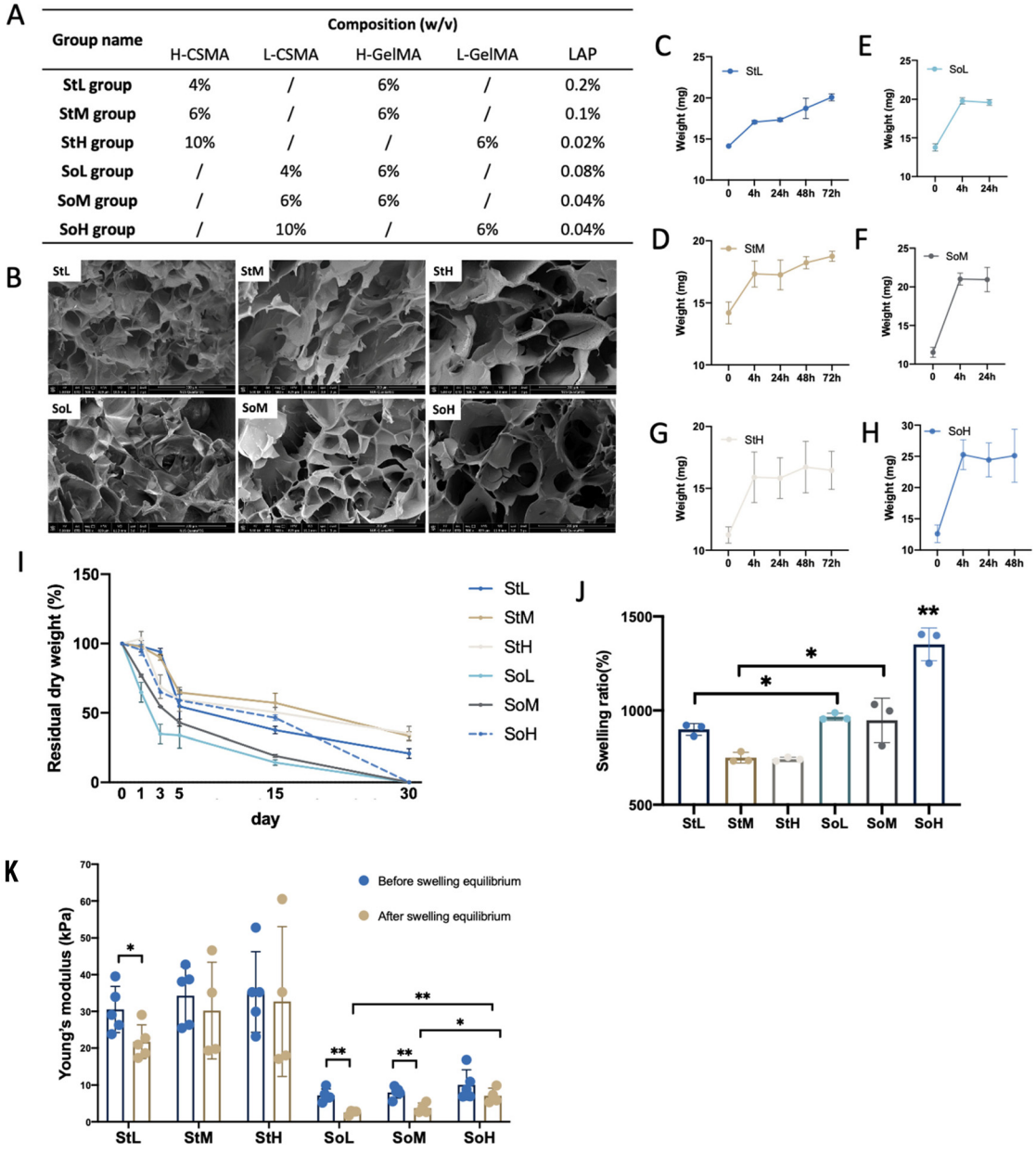

Fig. 3 Composition (A), morphology (B), swelling behaviour (C–H), degradation (I), swelling ratio (J) and Young's modulus (K) of each group. The comparison of Young's modulus before and after swelling equilibrium in each group was conducted by Student's *t*-test; the comparison of Young's modulus among the three stiff groups or the three soft groups before or after swelling equilibrium was conducted by one-way ANOVA followed by Tukey's *post hoc* test. The same method was applied to compare the swelling ratio among the six groups. $^{*}P < 0.05$, $^{**}P < 0.01$.

the SoL group and SoM group were found totally dissolved. All four samples in each soft group were found dissolved on day 30. While the stiff groups exhibited a sharp decline on the first 5 days, after that they degraded slowly and maintained a cylindrical shape until day 30. On day 30, the residual dry weight percentage for StL was significantly lower compared to the residual dry weight of the StM and StH groups, which were 20.78 ± 3.5%, 33.37 ± 2.94%, and 35.08 ± 5.19%, respectively. The swelling ratio of stiff hydrogels was lower than the swelling ratio of the corresponding soft groups (Fig. 3J) because the high DOF of polymers in stiff hydrogels increased the density of the cross-linking network thus restraining the penetration of water.[27,28] No significant difference in the swelling ratio was detected among the three stiff hydrogels, while the swelling ratio of the SoH group was significantly higher than that of the other five groups because L-CSMA, L-GelMA and low LAP concentration were used concurrently in this group.

As the swelling could affect Young's modulus of hydrogels, compressive tests were conducted upon UV crosslinking and after 24 h (Fig. 3K). As expected, Young's modulus of all groups decreased after swelling. There was no difference in Young's modulus between the three stiff groups after swelling. However, among the three soft groups, Young's modulus of SoH (7.10 ± 2.05 kPa) was significantly higher than that of the SoL group (2.53 ± 0.61 kPa) and the SoM group (3.74 ± 1.38 kPa) after swelling. The decrease of Young's modulus after swelling was more obvious in soft hydrogels probably due to their higher swelling ratio, because Young's modulus decreased with increased swelling of hydrogels.[29,30] The modulus in the StH and SoH groups showed a small decrease indicating that a higher mass fraction could help maintain Young's modulus.

3.4 Cell viability

MSCs were encapsulated in hydrogels and cultured in the chondrogenic differentiation medium for 28 days to compare the chondrogenesis of MSCs in each group (Fig. 4A). No difference in cell metabolism among the six groups was detected using AlamarBlue assay on day 1 (Fig. 4B). As shown in Fig. 4C, most encapsulated cells were alive (dyed in green) in each group and distributed homogeneously within the hydrogels, demonstrating the excellent biocompatibility of CSMA/

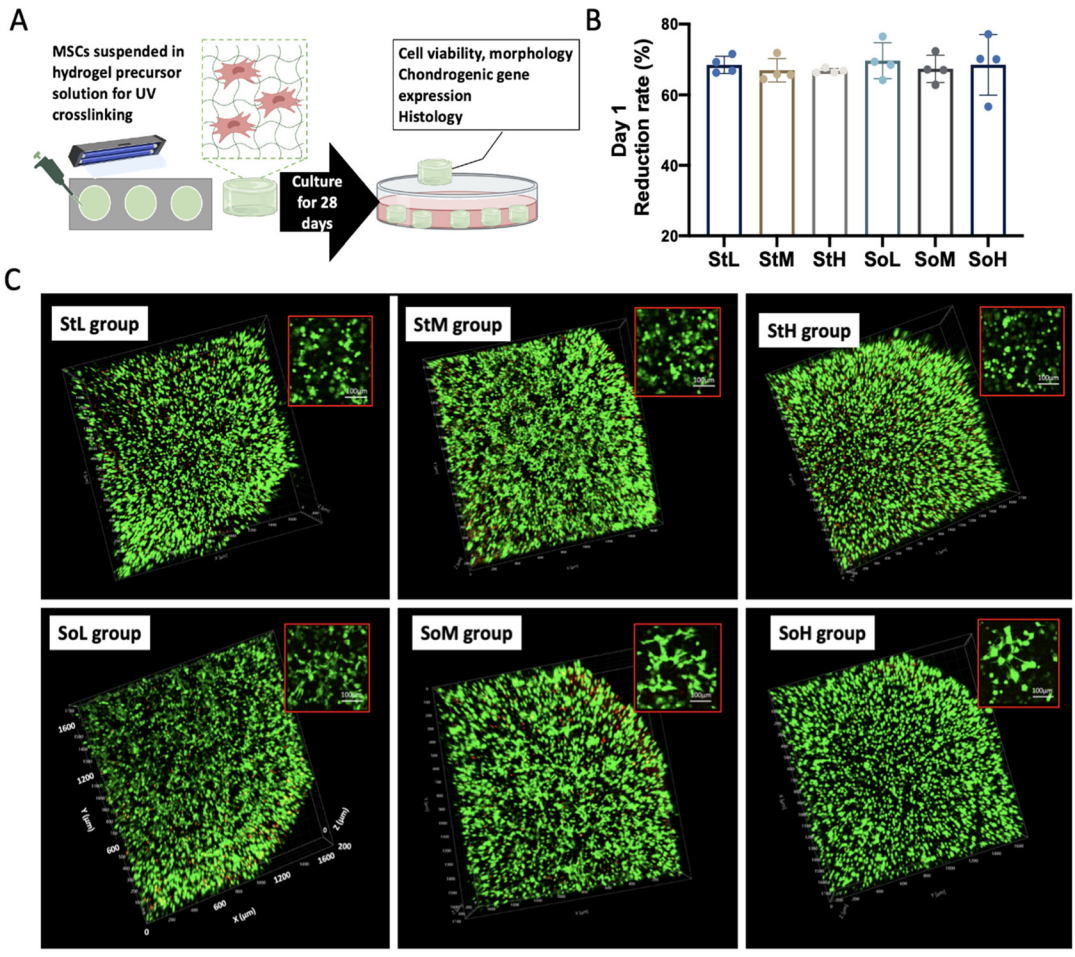

Fig. 4 Schematic overview of cell encapsulation in hydrogels for chondrogenesis (A); cell metabolism using AlamarBlue assay on day 1 (B); cell viability in each group using live/dead assay on day 1. Live cells are in green and dead cells in red (C).

GelMA hydrogels. In addition to cell viability, calcein AM staining could also provide cell morphological information. The cells encapsulated in stiff hydrogels remained round after culture for 24 hours, while some of the cells in the soft hydrogels spread and elongated as shown in the insets of Fig. 4C.

3.5 Cell morphology and metabolism

The morphology of MSCs in each group was further examined by phalloidin staining of F-actin after 2 weeks and 4 weeks of culturing in the chondrogenic differentiation medium (Fig. 5). In each group, cells located on the surface and the center of the hydrogel exhibited different morphologies. The cells on the surface elongated and aggregated on day 14 and day 28.

In comparison, cells were distributed separately in the center of hydrogels. On day 14, most of the cells spread out in all groups although more cells remained in a round shape in the StH and SoH groups which was probably due to the high mass fraction in these two groups restraining cell mobility. As the hydrogel degraded, more cellular projections were observed in the SoH group on day 28.

On day 28, a majority of cells in the center of stiff hydrogels exhibited a spherical morphology. However most of the cells in the center of soft hydrogels displayed stretched F-actin, which

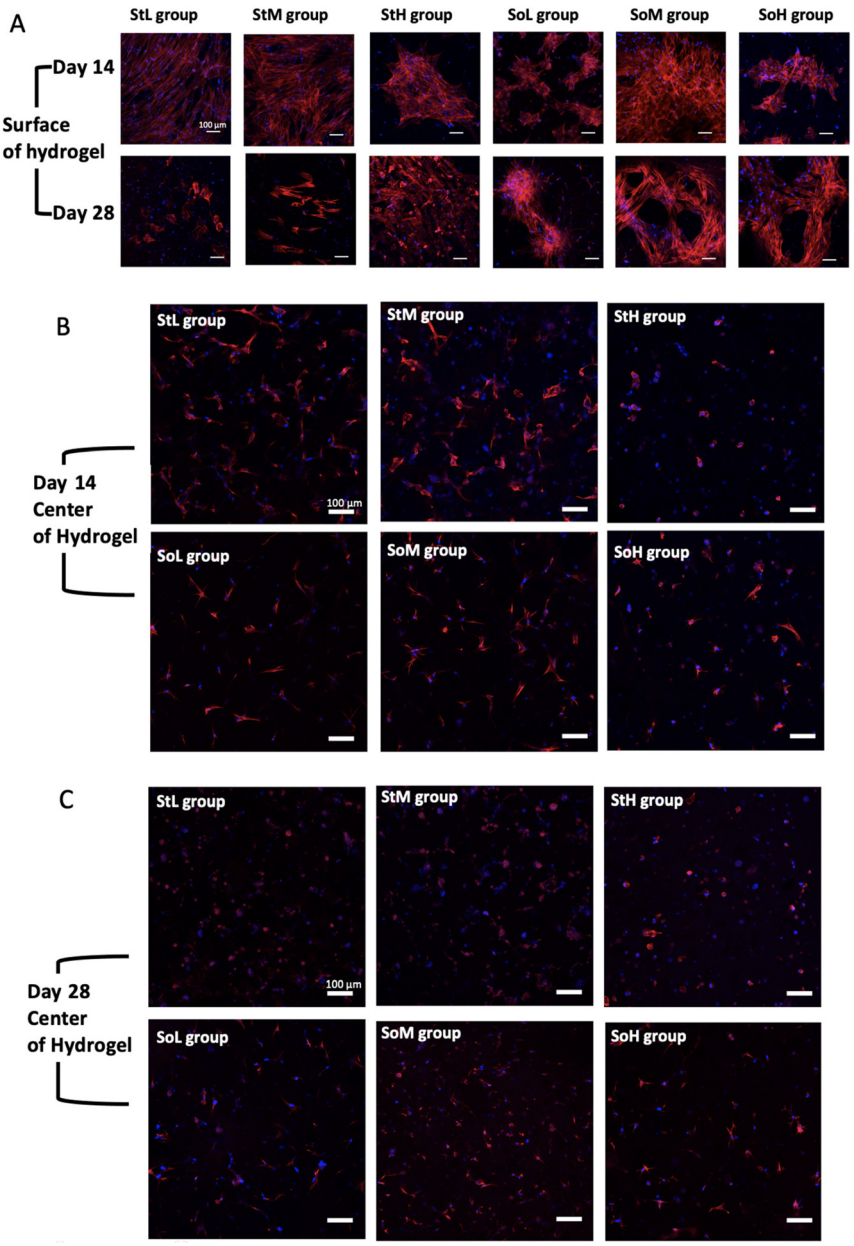

Fig. 5 Confocal laser microscopy images of MSCs stained with F-actin (red) and cell nuclei (blue) after being cultured for 14 days and 28 days in the chondrogenic differentiation medium. Cells on the surface of hydrogels on day 14 and day 28 (A); cells in the center of hydeogels on day 14 (B); cells in the center of hydrogels on day 28 (C).

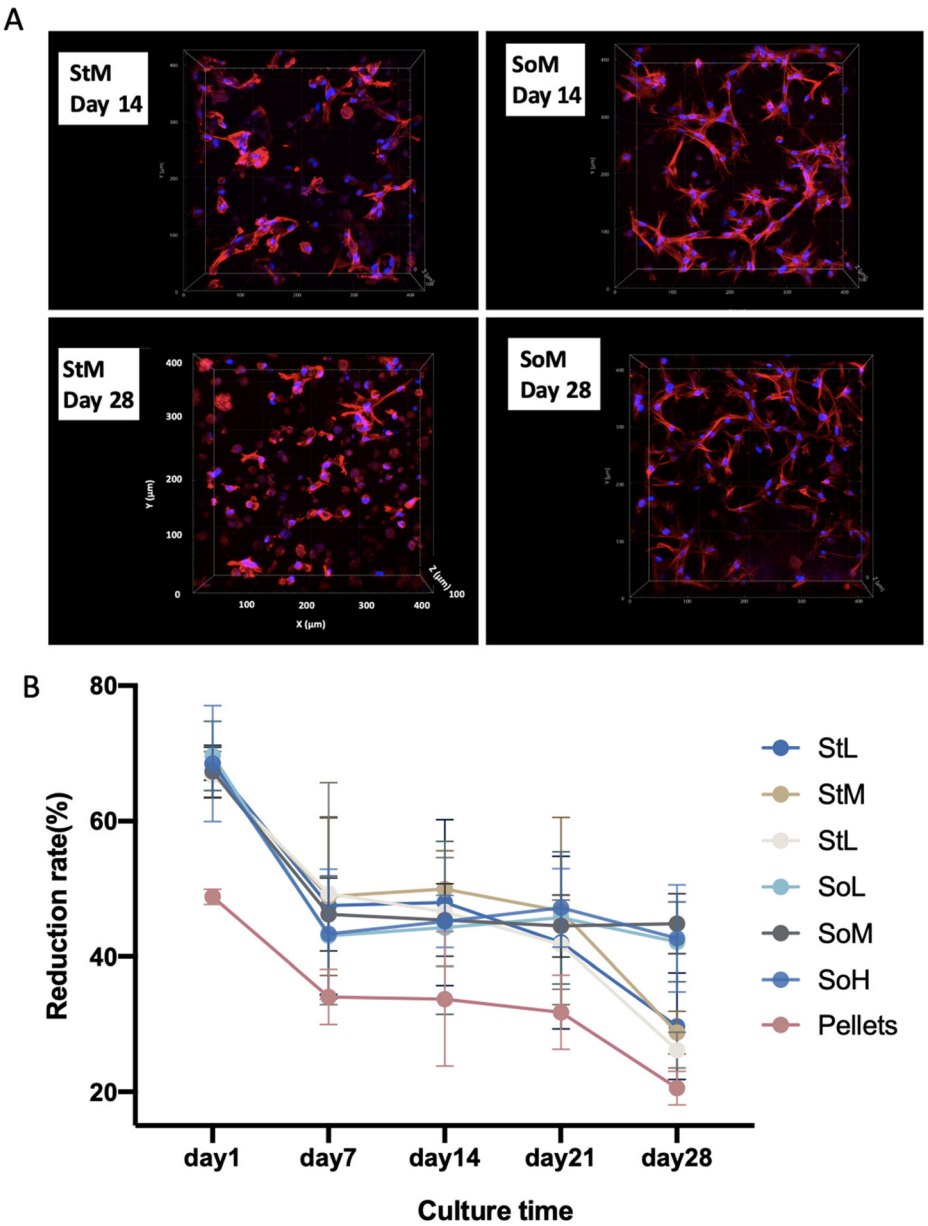

Fig. 6 (A) The Z-stack 3D reconstruction of the MSCs stained with F-actin (red) and cell nuclei (blue) after being cultured for 14 days and 28 days in the chondrogenic differentiation medium. (B) Cell metabolism during 28-day chondrogenic differentiation using AlamarBlue assay.

was demonstrated more clearly after Z-stack 3D reconstruction (Fig. 6A). Cellular protrusions in soft hydrogels maintained a finger-like structure, *i.e.* filopodium-like from day 14 to day 28, while most protrusions were wave-like extensions, *i.e.* lamellipodium-like in stiff hydrogels on day 14 and then transformed into a spherical shape on day 28.

For 28 days of culturing, the cell metabolic rate showed a decreasing trend in all groups of hydrogels and the pellet group (Fig. 6B). There was a sharp decrease from day 1 to day 7. Subsequently, in the soft groups the metabolism remained similar, while in the stiff groups and the pellet group, there was a significant decrease of metabolism from day 21 to day 28.

3.6 Gene expression analysis

Chondrogenesis of MSCs in each hydrogel group and the pellet group was evaluated by gene expression on day 14 and day 28 (Fig. 7A–F and ESI Fig. 1, 2†). The expression of SOX9, ACAN, and Col II increased from day 14 to day 28 while the expression of Col I decreased in all hydrogel groups. Two-way ANOVA with Tukey's *post hoc* comparison for SOX9, COMP, ACAN and Col II on day 28 demonstrated significance along both stiffness and CSMA concentration factors ($p < 0.05$). The higher mRNA expression level of chondrogenic markers in stiff hydrogels suggested that the overall chondrogenesis in stiff hydrogels was better than that in soft hydrogels (ESI Fig. 1†).

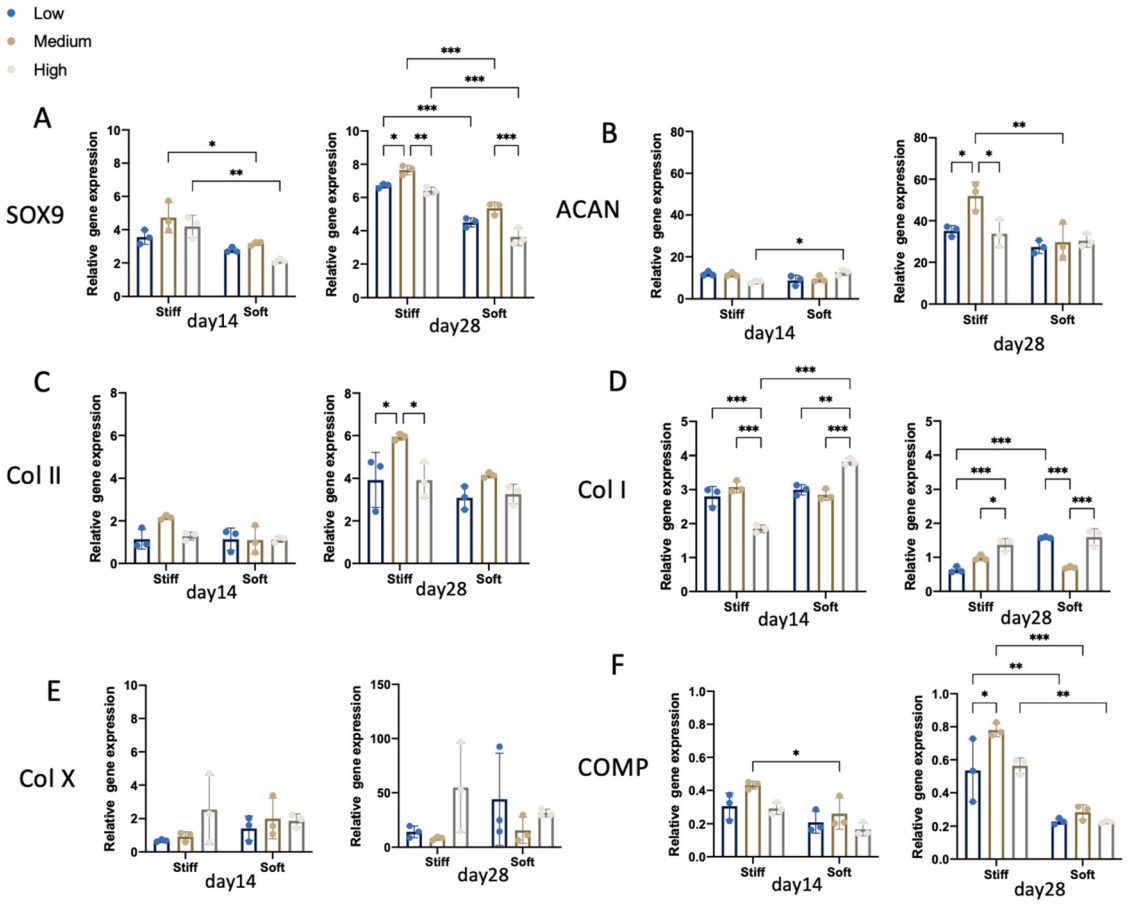

Fig. 7 Gene expression analysis in hydrogels. SOX9 (A), ACAN (B), Col II (C), Col I (D), Col X (E), COMP (F) gene expression of MSCs cultured in chondrogenic differentiation medium for 14 days and 28 days. Data presented as a fold difference relative to undifferentiated MSCs before encapsulation and normalized to GAPDH. Two-way ANOVA with Tukey's *post hoc* comparison for SOX9, COMP, ACAN, and Col II on day 28 demonstrated significance along both stiffness and CSMA concentration factors ($p < 0.05$). The significance of comparison among stiff or soft groups, and between the stiff group and soft group with the same CSMA concentration is marked. *$p < 0.05$, **$p < 0.01$, ***$p < 0.001$.

With the same CSMA concentration, the comparison between the stiff hydrogel and the soft hydrogel, especially StM *vs.* SoM, in Fig. 7A, B, and F supported that MSCs in stiff hydrogels exhibited better chondrogenic performance. In three stiff groups, SOX9 expression in StM was higher than in the other two groups on day 28; in three soft groups, the highest SOX9 expression was also observed in the group with medium CSMA content (SoM group). A similar trend was detected for the expression of ACAN, Col II, and COMP. The expression of hypertrophic marker Col X in the StM and the SoM groups on day 28 was lower although no statistical difference was detected. All these results indicated that the SoM group was optimal in the three soft groups and the StM group was optimal in the three stiff groups.

3.7 Histological evaluation of chondrogenesis

After culturing for 28 days, soft hydrogels were smaller in dimension than stiff hydrogels, as shown in ESI Fig. 3.† Because the hydrogel component CSMA as a sulfated glycosaminoglycan (GAG) could bind Alcian blue dyes, the newly formed GAG could not be compared by conventional Alcian blue staining (ESI Fig. 3†). In comparison, more GAG could be detected from day 14 to day 28 in chondrogenic pellets (ESI Fig. 4†).

Thus, immunohistochemical staining of SOX9 and Col II was conducted to compare the chondrogenesis in hydrogels (Fig. 8 and 9). Hydrogels without cell encapsulation were stained as the control to exclude unspecific staining due to the hydrogel component. The hydrogel itself, especially the soft hydrogels, displayed yellow colour. SOX9 is a transcriptional factor governing chondrogenic differentiation in mesenchymal stem cells. In fully differentiated chondrocytes, SOX9 is essentially confined to the nucleus. Thus, the true positive SOX9 signal in the hydrogel was dark brown and essentially nuclear.[31] Col II staining showed a much more intense signal in the cytoplasmic and extracellular area, compared to hydrogels without cell encapsulation as the control. The IHC staining results were consistent with the PCR findings. Two-way ANOVA with Tukey's *post hoc* comparison for SOX9 and Col II on day28 demonstrated significance along with stiffness and

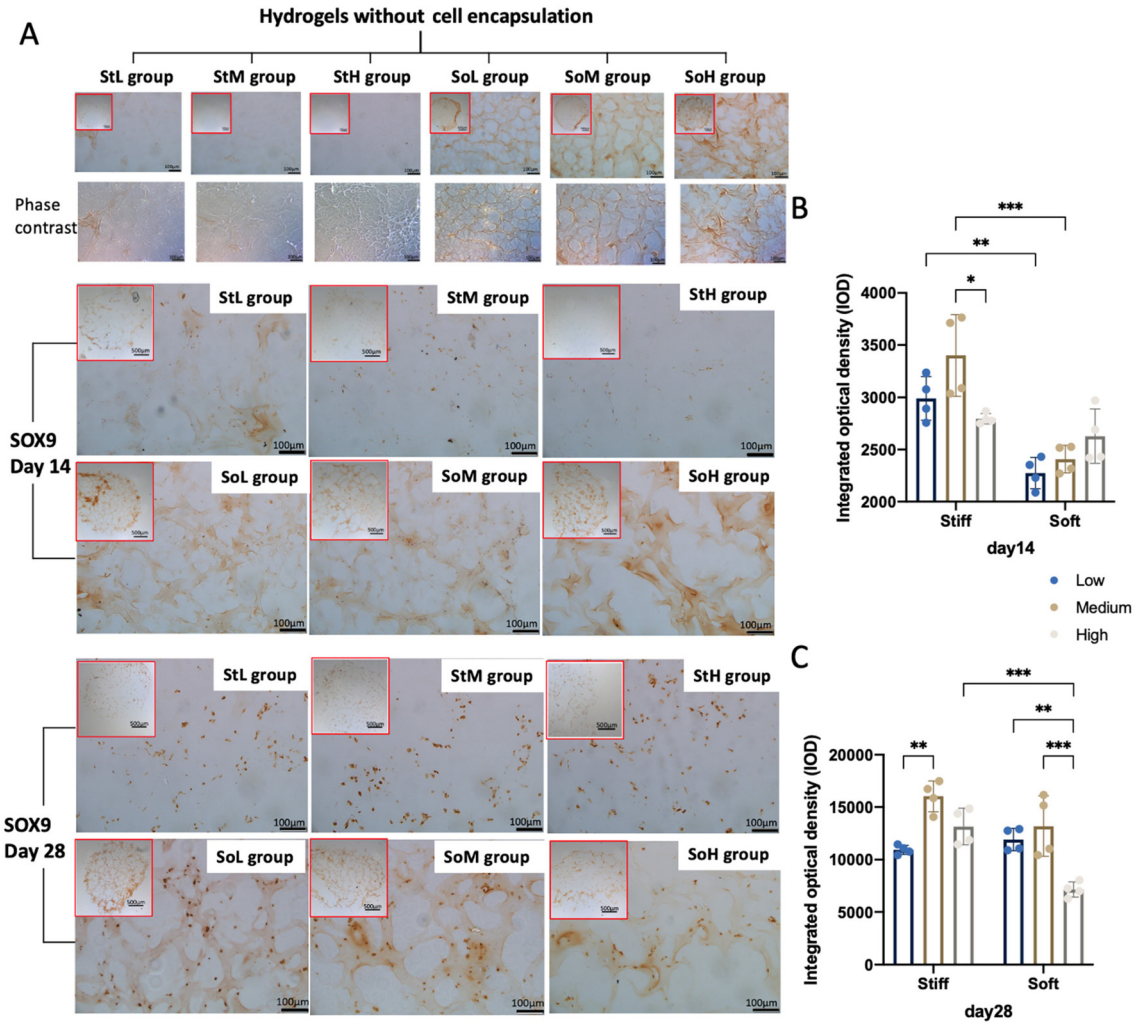

Fig. 8 SOX9 immunohistochemical staining of hydrogels after culture in chondrogenic differentiation medium for 14 days and 28 days. The images are at 200× magnification and the insets are at 40× magnification. Hydrogels without cell encapsulation were stained as control (A). Semi-quantification of Sox9 expression in each group on day 14 (B). Semi-quantification of Sox9 expression in each group on day 28 (C). The comparison of semi-quantification results was conducted by two-way ANOVA followed by Tukey's *post hoc* test. The significance of comparison among stiff or soft groups, and between the stiff group and soft group with the same CSMA concentration is marked *$p < 0.05$, **$p < 0.01$, ***$p < 0.001$.

CSMA concentration factors ($p < 0.05$). The most intense staining of SOX9 and Col II was detected in the StM group on both day 14 and day 28, and the second highest Col II signal was detected in the SoM group.

3.8 Young's modulus of hydrogels after culture for 28 days

After culturing for 28 days in the chondrogenic differentiation medium, Young's modulus of hydrogels was measured by compressive tests. As shown in Fig. 10A and B, after 28-day culture, Young's modulus of the SoM group was higher than that of all the other groups. The SoL and StL groups were too soft to break during compression. In stiff hydrogels, the StM had a significantly higher Young's modulus than the StL and StH groups. Compared to the Young's modulus of hydrogels without cell encapsulation upon swelling equilibrium, all groups exhibited a significant decrease except for the SoM group (Fig. 10C). The average Young's modulus of the three groups without cell encapsulation after swelling was 28.58 ± 13.03 kPa and 4.46 ± 2.31 kPa for the stiff groups and soft groups respectively. The Young's modulus decreased sharply in the stiff groups compared to hydrogels without cell encapsulation (Fig. 10C). The Young's moduli for StL, StM, and StH were 0.64 ± 0.33 kPa, 2.55 ± 0.39 kPa, and 0.77 ± 0.19 kPa, respectively. In soft hydrogels, the moduli of SoL and SoH also decreased. In contrast, the modulus of the SoM group was slightly increased after 28-day culture (3.74 ± 1.35 kPa *vs.* 5.39 ± 1.31 kPa, $P = 0.202$).

In terms of the volume of hydrogels (Fig. 10D), stiff groups did not show significant changes, while the volume of the StH group increased probably because the mesh size increased along with the decreasing crosslinking density due to degradation so that more water could penetrate into the hydrogel.

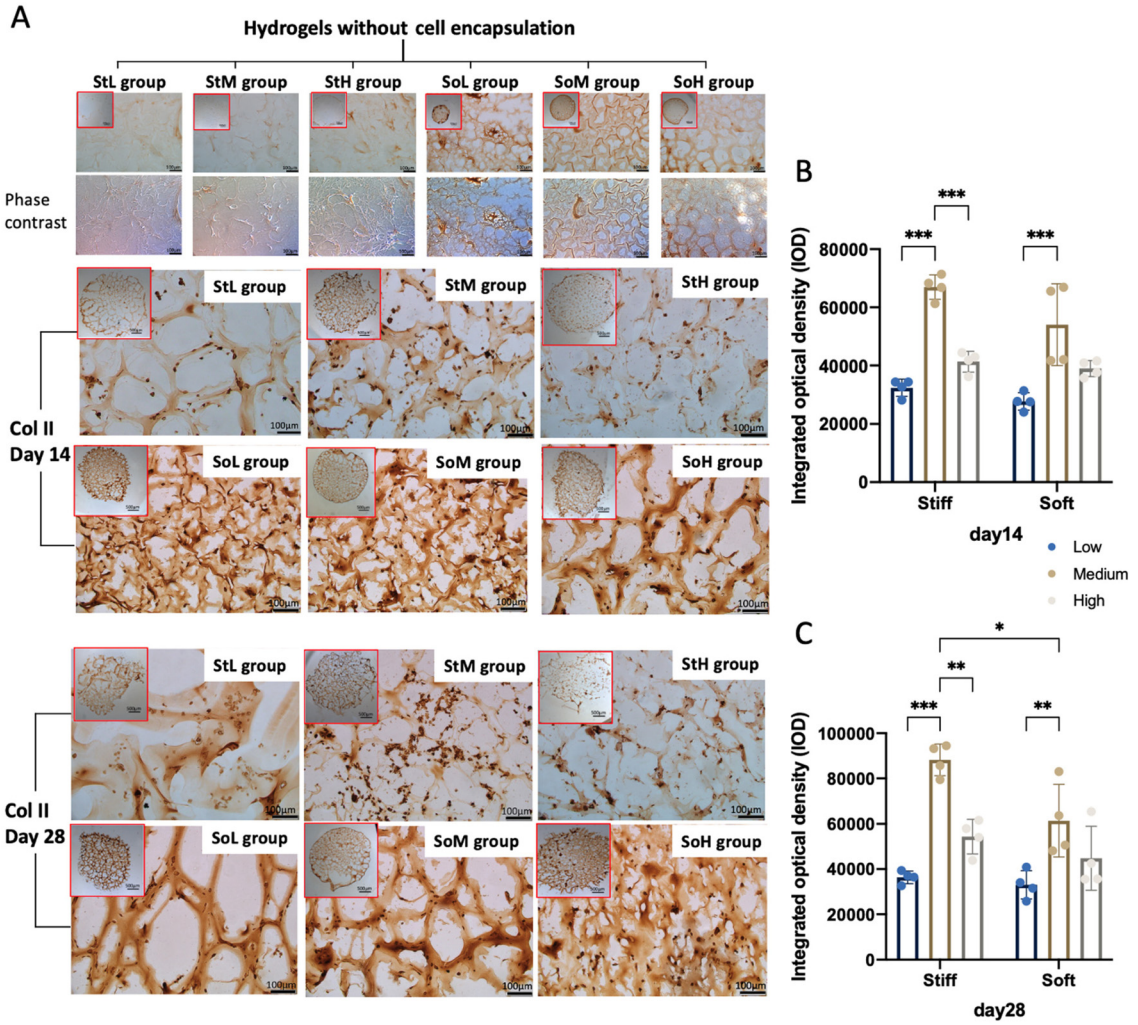

Fig. 9 Col II immunohistochemical staining of hydrogels after culture in chondrogenic differentiation medium for 14 days and 28 days. The images are at 200× magnification and the insets are at 40× magnification. Hydrogels without cell encapsulation were stained as control (A). Semi-quantification of Col II expression in each group on day 14 (B). Semi-quantification of Col II expression in each group on day 28 (C). The comparison of semi-quantification results was conducted by two-way ANOVA followed by Tukey's *post hoc* test. The significance of comparison among stiff or soft groups, and between the stiff group and soft group with same CSMA concentration is marked *$p < 0.05$, **$p < 0.01$, ***$p < 0.001$.

However in the soft groups, all groups showed a decrease in volume, suggesting degradation that caused hydrogel dissolving was predominant. The change of Young's modulus, volume, and cellular morphology in hydrogels are shown in Fig. 10E.

4. Discussion

In this study, the experimental design incorporated different matrix stiffness and gradient CSMA concentrations. The CSMA/GelMA hydrogels were tuned to the predefined stiffness by adjusting the DOF and LAP concentration, thus providing a platform to investigate how stiffness and CSMA concentration affect the chondrogenesis of MSCs. Interestingly, the StM group exhibited the best chondrogenesis among the three stiff groups (33.36 ± 8.25 kPa). Likewise, in the three soft groups (8.42 ± 2.83 kPa) the SoM group supported superior chondrogenesis of MSCs than the SoL and SoH groups. Furthermore, given the same CSMA concentration, better chondrogenesis of MSCs was observed in the stiff hydrogels compared to the soft group.

The swelling ratio and degradation rate of soft hydrogels were higher than those of the stiff groups because the DOF of CSMA and GelMA in the soft groups were lower. In the swelling test, after being immersed in PBS for 48 h, the soft hydrogels became too soft to be transferred; in the degradation test, all soft hydrogels were found to dissolve after 30 days in PBS. GelMA is both enzymatically and hydrolytically degradable. It contains both gelatin methacrylate and methacrylamide groups, and methacrylate groups represented less than 10% of all methacryloyl substitutions.[26] Despite the methacrylate

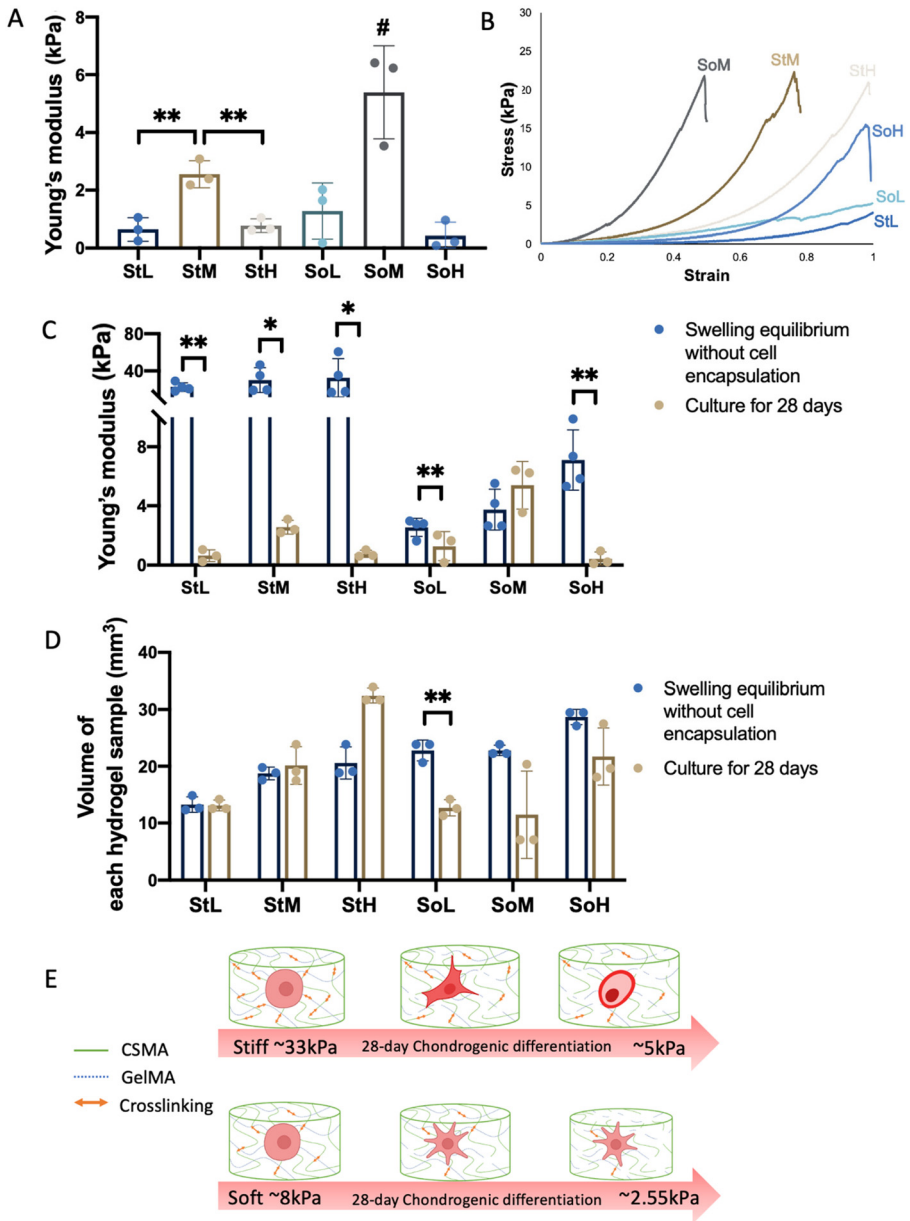

Fig. 10 (A) Young's modulus of hydrogels in each group after culture for 28 days in the chondrogenic differentiation medium. The comparison among six groups was conducted by one-way ANOVA followed by Turkey's multiple comparisons, $^{\#}p < 0.05$; the comparison among stiff hydrogels (StL, StM, StH groups) was conducted in the same way, $^{**}p < 0.01$. (B) The representative strain–stress curve of each group; (C) Young's modulus of hydrogels without cell encapsulation and cell-laden hydrogels cultured for 28 days. The comparison in each group was conducted by Student's *t*-test. $^{*}p < 0.05$, $^{**}p < 0.01$. (D) The volume of hydrogels after swelling equilibrium without cell encapsulation and hydrogels after culture for 28 days in the chondrogenic differentiation medium, which comparison was conducted by Student's *t*-test. $^{**}p < 0.01$. (E) Illustration of hydrogel degradation and cellular morphology in stiff and soft hydrogels along chondrogenesis.

groups being stable, the methacrylamide groups of GelMA decomposed within 3 h in an alkaline solution.[32] As for CSMA, the methacrylate ester bonds in the CSMA hydrogel were also prone to hydrolyse in the physiological buffer at 37 °C.[33] The DoF of GelMA and CSMA used in the soft hydrogels was lower so that they hydrolytically degraded faster than the stiff hydrogels in the degradation test. Although without cell encapsulation the soft hydrogels were totally degraded in PBS after 30 days, with cell encapsulation the soft hydrogels maintained a clear cylindrical shape after 28-day chondrogenic differentiation (Fig. S2†). The reason could be that encapsulated cells could exert contractile forces on polymer chains.[34] These contractile forces could help maintain the shape of the crosslinked hydrogels; in addition, the ECM secreted by the encapsulated cells also slowed the degradation.[35]

The cells encapsulated in hydrogels displayed two distinct morphologies on the surface and in the center (Fig. 5). This was probably because the cells in the center sensed a homo-

geneous hydrogel environment, while the cells close to the surface of the hydrogel were conditioned by two microenvironments: the cell culture medium and the hydrogel. The difference in biochemical cues and mechanical stimulus caused the cells at the interface of medium and hydrogel to be stretched and aggregated similar to cells proliferated on a 2D substrate.[36] After 14 days and 28 days, cell aggregates were clearly observed on the surface of hydrogels, but no comparable aggregates were found in the center of hydrogels. This suggested that the mobility of cells on the surface was better than that of cells in the center probably because the homogeneous 3D environment in the center of hydrogels limits cellular migration.

Cells elongated faster in soft hydrogels as shown by live/dead staining on day 1 (Fig. 4) probably because degradation was faster, and lower crosslinking density in the soft groups made the polymer chains more pliable, facilitating the cell spreading.[37–39] On day 14, the cellular protrusions in stiff hydrogels were dominantly lamellipodia-like but in soft hydrogels were filopodia-like. Lamellipodia, wave-like extensions of the plasma membrane, contained densely packed branched actin filaments and were regarded as the main force driving mesenchymal cell migration; filopodia, finger-like structures, were composed of linear actin filaments and served as cellular antennas sensing chemical or mechanical cues.[40] Both forms of actin machinery functioned together at the leading edge of cells to facilitate cell migration. Our findings were consistent with previous studies which proved that increased stiffness could benefit the stability of lamellipodia and decrease the number of filopodia protrusions extending from a cell.[41,42] During cell spreading, filopodia were responsible for the initial rigidity sensing followed by the spreading of lamellipodia.[42] After the filopodia touched the cell binding sequence in the matrix and formed a nascent focal complex, the resistance from the rigid matrix caused the nascent adhesion to mature into focal adhesion and projections to expand to form stable lamellipodia, while the soft matrix was pliable resulting in a weak cell–matrix bond that was unfavorable for adhesion stabilization.[41,42] Our results indicated that a more stable connection force in the morphology of lamellipodia favoured chondrogenesis. In contrast, Aprile *et al.* reported that soft hydrogel environments facilitated cell spreading and aggregation thus preferentially supporting chondrogenesis of stem cells.[43] In their study, higher stiffness of hydrogels was achieved by increasing the concentration of agarose in the collagen I/agarose hydrogel. As we found in the present study, fewer cell protrusions in the StH and SoH groups on day 14 were observed (Fig. 5B), suggesting that a higher mass fraction in the hydrogel was disadvantageous to cell spreading. In Aprile *et al.*'s study, the limitation of cell spreading in stiff hydrogels could be due to the higher mass fraction in the stiff hydrogels than in soft hydrogels, rather than the function of stiffness itself.

In the soft or stiff groups, the StM and SoM groups composed of 6% CSMA and 6% GelMA showed better chondrogenesis than other groups composed of 4% or 10% CSMA and 6% GelMA. Despite many studies which have verified that CS could help to create a chondro-inductive environment for the encapsulated stem cells,[12,13,44] the detailed mechanism behind this function is still not clear. In a hydrogel system, the environmental cues that regulate stem cell behavior may come from structural crosslinking density or direct cellular interactions with some biochemical signals.[37] One possible explanation for the finding of this study was that the combination of 6% GelMA and 6% CSMA built the most appropriate physical environment for cellular spreading, migration, and differentiation during chondrogenesis. The other possible explanation could be that CS, as a negatively charged glycosaminoglycan, could bind positively charged growth factors electrostatically,[45,46] thus controlling the local concentration of growth factors and facilitating early chondrogenesis.[44] It has been shown that in the skeletal development the sulfation of GAG fostered direct cell–proteoglycan interactions with specific growth factors or signalling molecules such as transforming growth factor (TGFβ), bone morphogenic proteins (BMPs), Indian hedgehog (IHH), parathyroid hormone-related peptide (PTHrP).[14] Wang *et al.*[18] found the optimal CS concentration for chondrogenesis was 5% among the various concentrations (0%, 2%, 5%, 7.5%, and 10%) in the CS/PEG hydrogel. In another study, Rogan *et al.*[47] incorporated varying concentrations of CSMA (3%, 6%, 9%) with 8% gelatin microribbons and found that the optimal concentration of CSMA was 6% to support chondrogenesis of the co-culture of adipose-derived stem cells and neonatal chondrocytes. These findings suggested that 5% or 6% CSMA led to optimal chondrogenesis regardless of other components and mass fraction of the hydrogels. Therefore, 6% CSMA showed superiority in terms of chondrogenesis over 4% or 10% mostly because this density of sulfation was optimal for its interaction with cells.

The overall observations in this study suggest that the chondrogenesis in stiff hydrogels was better than that in soft hydrogels. From the perspective of morphology, during chondrogenesis, MSCs transformed from a stretched morphology to a spherical morphology.[48] From cytoskeleton staining (Fig. 5 and 6A), on day 28, most cells in stiff hydrogels displayed a spherical shape, while cells in soft hydrogels were still elongated with filopodia on the edge. From the view of cell metabolism change, the metabolism of chondrogenic differentiating shifted from an oxidative-dominant to a glycolytic-dominant state with significantly reduced oxygen consumption.[49,50] The reduction rate detected by the AlamarBlue assay showed a decreasing trend (Fig. 6B) but the significant decrease from day 21 to day 28 was only observed in stiff groups and pellets, indicating better chondrogenic differentiation progression in these groups. The PCR results also confirmed the superior chondrogenic differentiation in stiff hydrogels as observed from the mRNA expression of chondrogenic markers SOX9, aggrecan, collagen II and COMP (Fig. 7 and ESI Fig. 1†). The IHC results of SOX9 and Col II also confirmed the superiority of chondrogenesis in stiff hydrogels, especially in the StM group (Fig. 8 and 9).

The effect of matrix stiffness on chondrogenesis has long been studied in hydrogel systems, but results were inconsistent

and inconclusive. For example, lower crosslinked hyaluronic acid–tyramine hydrogel with Young's modulus of 5.4 kPa,[51] polyvinyl alcohol/hyaluronic acid hydrogel with a modulus of 80 kPa in the range between 20 kPa and 200 kPa,[52] softer GelMA with a storage modulus of 0.5 kPa[53] were reported to show the optimal chondrogenic differentiation of stem cells. Sun *et al.* found in [poly-D,L-lactic acid/polyethylene glycol/poly-D,L-lactic acid] (PDLLA–PEG) hydrogel material that concentration affects chondrogenesis rather than material stiffness.[54] Wang *et al.* found that in soft hydrogels with Young's modulus of 3 kPa, an increase of hyaluronic acid from 0.5% to 5% resulted in the upregulation of Col II in a dose-dependent manner, but this trend was reversed in stiff hydrogels with Young's modulus of 90 kPa.[55] These diverse findings dictated the hurdle to interpreting the role of matrix stiffness in chondrogenesis. In our view, one significant reason for this hurdle is that when using hydrogels to study the relationship between stiffness and chondrogenesis in a 3D environment, it is difficult to maintain stiffness as an independent variable because hydrogel stiffness is linked to other properties such as crosslinking density,[51] degradation rate,[54] mass fraction,[55] *etc*. These properties could affect cellular behavior such as spreading, proliferation and migration, as well as the mechanosensing pathway. In this study, the stiffness difference was controlled by modifying the DoF of polymers and the concentration of photoinitiator LAP without altering the mass fraction of individual components (*i.e.* CS and gelatin). This could affect the crosslinking density and degradation rate, thus affecting cell spreading and migration, and possibly leading to different chondrogenic performances. Therefore, in the studies using hydrogels to investigate the effect of stiffness on the chondrogenesis of stem cells in a 3D environment, the term "stiffness" may represent an integrative variable from matrix elasticity, degradation rate, crosslinking density, *etc*. In tissue engineering application, the specific optimization of "stiffness" for each hydrogel is necessary because a general optimal stiffness value may not exist.

Meanwhile, it should be taken into consideration that the stiffness is dynamic in degradable hydrogels. After 28-day differentiation, the moduli of each group decreased except for the SoM group; particularly in the stiff groups, the modulus dropped from around 25 kPa to less than 3 kPa. CSMA and GelMA underwent hydrolytic and proteolytic degradation along with the chondrogenesis of stem cells and cellular matrix deposition. In the stiff groups, the maintenance and increase of volume (Fig. 10D) was probably due to less mass loss of CSMA and GelMA and reduced crosslinking density that allowed more water penetration. However in the soft groups, the volume decreased because the degradation process separated more CSMA or GelMA chains from the hydrogel. Such mass loss reduced the volume of the hydrogel. In stiff hydrogels, decreased crosslinking density outweighed the cellular matrix deposition and the moduli of all three groups dropped significantly (Fig. 10C). The modulus of the StM group was higher than that of StL and StH groups due to its superior chondrogenic performance generating more cellular matrix deposition. In the soft hydrogels, the increased pliability of GelMA and CSMA made the hydrogel more likely to shrink due to the contraction force exerted by cells.[41,56] The cellular contraction and matrix deposition maintained Young's modulus of the SoM group. In turn, the change of hydrogel modulus demonstrated that the mechanical cues in the CSMA/GelMA hydrogel system were dynamic depending on the degradation, cellular matrix deposition, and pliability of polymer chains.[41,57] This could be the reason for the contradictory findings between this study and Wang *et al.*'s study. In Wang *et al.*'s study[18] 7.5 kPa was better for chondrogenesis compared to 36 kPa using the CS/PEG hydrogel as PEG was not degradable. However, in this study the initial modulus of 33 kPa was preferred for chondrogenesis because the mechanical stimulus was dynamically decreasing due to the degradation of GelMA and CSMA. This suggested both the initial stiffness and the dynamic stiffness along differentiation could affect chondrogenesis.

Some limitations were noted in this study. In this experimental setup, even though high-DOF CSMA and high-DOF GelMA both were used for hydrogel preparation, the high stiffness value that could be achieved was less than 40 kPa. Since this study demonstrated that stiff hydrogels performed better, in the future study other polymers could be incorporated to investigate the performance of stiffer CS-containing hydrogels. Additionally, Col X expression was upregulated from day 14 to day 28 in all groups, indicating the presence of hypertrophy in chondrogenesis. Further study aimed at inhibiting hypertrophy is needed. Aisenbrey *et al.*[14] demonstrated that CS with dynamic loading could create physiochemical cues supporting chondrogenesis and attenuating hypertrophy, which could be a promising direction. Meanwhile, no obvious cell aggregation was observed in the center of the hydrogel compared to the surface of the hydrogel. This indicated that the cell migration in the hydrogel was restrained by the polymer network. Therefore, further modification of the hydrogel, such as incorporating peptides,[58,59] using microchannel networks,[60] *etc.* is needed to facilitate cell aggregation in the center of the hydrogel.

5. Conclusion

To summarize, this study demonstrated that both CSMA concentration and stiffness of hydrogels affected chondrogenesis in CSMA/GelMA hydrogels. Regarding CSMA concentration, the medium concentration 6% (w/v) supported better chondrogenesis of MSCs compared to the low 4% (w/v) and high 10% (w/v) concentrations of CSMA regardless of stiffness. Comparing the soft hydrogel group with the stiff hydrogel group of the same CSMA concentration, MSCs in the stiff hydrogel exhibited a trend of superior chondrogenesis. This study presents an advancement in the optimization of CSMA concentration and stiffness of hydrogels for chondrogenesis. In the CSMA/GelMA hydrogel, 6% (w/v) CSMA with an initial Young's modulus around 33 kPa is recommended for cartilage tissue engineering.

Author contributions

C. C. Ai: conceptualization, data curation, formal analysis, investigation, methodology, validation, visualization, and writing the original draft; J. C. H. Goh: funding acquisition, project administration, and supervision; L. Liu: conceptualization, methodology, and visualization; X. H. Tan: conceptualization, investigation, and methodology; K. Wong: investigation and methodology. All the authors contributed to reviewing and editing the final version of the manuscript.

Conflicts of interest

There are no conflicts of interest to declare.

Acknowledgements

This work was funded by the National Research Foundation (NRF) Central Gap Funding – TGIIT18may0011.

References

1 T. M. Simon and D. W. Jackson, *Sports Med. Arthrosc. Rev.*, 2018, **26**, 31–39.
2 W. Widuchowski, J. Widuchowski and T. Trzaska, *Knee*, 2007, **14**, 177–182.
3 S. H. Kim, D. Y. Park and B.-H. Min, *Tissue Eng. Regener. Med.*, 2012, **9**, 240–248.
4 Y. Na, Y. Shi, W. Liu, Y. Jia, L. Kong, T. Zhang, C. Han and Y. Ren, *Int. J. Surg.*, 2019, **68**, 56–62.
5 E. C. Rodríguez-Merchán, *Am. J. Orthop.*, 2012, **41**, 236–239.
6 E. V. Medvedeva, E. A. Grebenik, S. N. Gornostaeva, V. I. Telpuhov, A. V. Lychagin, P. S. Timashev and A. S. Chagin, *Int. J. Mol. Sci.*, 2018, **19**, 2366.
7 B. Balakrishnan and R. Banerjee, *Chem. Rev.*, 2011, **111**, 4453–4474.
8 S. Sant, M. J. Hancock, J. P. Donnelly, D. Iyer and A. Khademhosseini, *Can. J. Chem. Eng.*, 2010, **88**, 899–911.
9 P. A. Levett, F. P. Melchels, K. Schrobback, D. W. Hutmacher, J. Malda and T. J. Klein, *Acta Biomater.*, 2014, **10**, 214–223.
10 J. M. Coburn, M. Gibson, S. Monagle, Z. Patterson and J. H. Elisseeff, *Proc. Natl. Acad. Sci. U. S. A.*, 2012, **109**, 10012–10017.
11 X. Li, Q. Xu, M. Johnson, X. Wang, J. Lyu, Y. Li, S. McMahon, U. Greiser, S. A and W. Wang, *Biomater. Sci.*, 2021, **9**, 4139–4148.
12 B. Corradetti, F. Taraballi, S. Minardi, J. Van Eps, F. Cabrera, L. W. Francis, S. A. Gazze, M. Ferrari, B. K. Weiner and E. Tasciotti, *Stem Cells Transl. Med.*, 2016, **5**, 670–682.
13 G. Bauza-Mayol, M. Quintela, A. Brozovich, M. Hopson, S. Shaikh, F. Cabrera, A. Shi, F. B. Niclot, F. Paradiso and E. Combellack, *Adv. Healthcare Mater.*, 2022, **11**, 2101127.
14 E. A. Aisenbrey and S. J. Bryant, *Biomaterials*, 2019, **190**, 51–62.
15 D.-A. Wang, S. Varghese, B. Sharma, I. Strehin, S. Fermanian, J. Gorham, D. H. Fairbrother, B. Cascio and J. H. Elisseeff, *Nat. Mater.*, 2007, **6**, 385–392.
16 J. Zhang, B. Li, J. Zuo, R. Gu, B. Liu, C. Ma, J. Li and K. Liu, *Adv. Healthcare Mater.*, 2021, **10**, 2100109.
17 J. H. Wen, L. G. Vincent, A. Fuhrmann, Y. S. Choi, K. C. Hribar, H. Taylor-Weiner, S. Chen and A. J. Engler, *Nat. Mater.*, 2014, **13**, 979–987.
18 T. Wang and F. Yang, *Stem Cell Res. Ther.*, 2017, **8**, 284.
19 L. Han, M. Wang, P. Li, D. Gan, L. Yan, J. Xu, K. Wang, L. Fang, C. W. Chan, H. Zhang, H. Yuan and X. Lu, *ACS Appl. Mater. Interfaces*, 2018, **10**, 28015–28026.
20 P. A. Janmey, D. A. Fletcher and C. A. Reinhart-King, *Physiol. Rev.*, 2020, **100**, 695–724.
21 L. Bian, C. Hou, E. Tous, R. Rai, R. L. Mauck and J. A. Burdick, *Biomaterials*, 2013, **34**, 413–421.
22 D. Loessner, C. Meinert, E. Kaemmerer, L. C. Martine, K. Yue, P. A. Levett, T. J. Klein, F. P. Melchels, A. Khademhosseini and D. W. Hutmacher, *Nat. Protoc.*, 2016, **11**, 727–746.
23 K. J. Ornell, D. Lozada, N. V. Phan and J. M. Coburn, *J. Mater. Chem. B*, 2019, **7**, 2151–2161.
24 L.-F. Wang, S.-S. Shen and S.-C. Lu, *Carbohydr. Polym.*, 2003, **52**, 389–396.
25 E. Hoch, T. Hirth, G. E. Tovar and K. Borchers, *J. Mater. Chem. B*, 2013, **1**, 5675–5685.
26 K. Yue, X. Li, K. Schrobback, A. Sheikhi, N. Annabi, J. Leijten, W. Zhang, Y. S. Zhang, D. W. Hutmacher and T. J. Klein, *Biomaterials*, 2017, **139**, 163–171.
27 X. Li, S. Chen, J. Li, X. Wang, J. Zhang, N. Kawazoe and G. Chen, *Polymers*, 2016, **8**, 269.
28 J. W. Nichol, S. T. Koshy, H. Bae, C. M. Hwang, S. Yamanlar and A. Khademhosseini, *Biomaterials*, 2010, **31**, 5536–5544.
29 B. Johnson, D. Beebe and W. Crone, *Mater. Sci. Eng., C*, 2004, **24**, 575–581.
30 R. Subramani, A. Izquierdo-Alvarez, P. Bhattacharya, M. Meerts, P. Moldenaers, H. Ramon and H. Van Oosterwyck, *Front. Mater.*, 2020, **7**, 212.
31 V. Lefebvre, W. Huang, V. R. Harley, P. N. Goodfellow and B. de Crombrugghe, *Mol. Cell. Biol.*, 1997, **17**, 2336–2346.
32 J. Zheng, M. Zhu, G. Ferracci, N.-J. Cho and B. H. Lee, *Macromol. Chem. Phys.*, 2018, **219**, 1800266.
33 C. C. L. Schuurmans, A. J. Brouwer, J. A. W. Jong, G.-J. P. H. Boons, W. E. Hennink and T. Vermonden, *ACS Omega*, 2021, **6**, 26302–26310.
34 C. Lee, A. Grodzinsky and M. Spector, *Biomaterials*, 2001, **22**, 3145–3154.
35 S. Krishnamoorthy, B. Noorani and C. Xu, *Int. J. Mol. Sci.*, 2019, **20**, 5061.
36 Y. Ma, M. Lin, G. Huang, Y. Li, S. Wang, G. Bai, T. J. Lu and F. Xu, *Adv. Mater.*, 2018, **30**, 1705911.
37 S. Khetan, M. Guvendiren, W. R. Legant, D. M. Cohen, C. S. Chen and J. A. Burdick, *Nat. Mater.*, 2013, **12**, 458–465.
38 A. M. Kloxin, A. M. Kasko, C. N. Salinas and K. S. Anseth, *Science*, 2009, **324**, 59–63.

39 N. Huebsch, P. R. Arany, A. S. Mao, D. Shvartsman, O. A. Ali, S. A. Bencherif, J. Rivera-Feliciano and D. J. Mooney, *Nat. Mater.*, 2010, **9**, 518–526.
40 M. Innocenti, *Cell Adhes. Migr.*, 2018, **12**, 401–416.
41 P. W. Oakes, T. C. Bidone, Y. Beckham, A. V. Skeeters, G. R. Ramirez-San Juan, S. P. Winter, G. A. Voth and M. L. Gardel, *Proc. Natl. Acad. Sci. U. S. A.*, 2018, **115**, 2646–2651.
42 S. Wong, W.-H. Guo and Y.-L. Wang, *Proc. Natl. Acad. Sci. U. S. A.*, 2014, **111**, 17176–17181.
43 P. Aprile, I. T. Whelan, B. N. Sathy, S. F. Carroll and D. J. Kelly, *Macromol. Biosci.*, 2022, **22**, e2100365.
44 S. Varghese, N. S. Hwang, A. C. Canver, P. Theprungsirikul, D. W. Lin and J. Elisseeff, *Matrix Biol.*, 2008, **27**, 12–21.
45 M. C. Goude, T. C. McDevitt and J. S. Temenoff, *Cells Tissues Organs*, 2014, **199**, 117.
46 C. I. Gama, S. E. Tully, N. Sotogaku, P. M. Clark, M. Rawat, N. Vaidehi, W. A. Goddard, A. Nishi and L. C. Hsieh-Wilson, *Nat. Chem. Biol.*, 2006, **2**, 467–473.
47 H. Rogan, F. Ilagan, X. Tong, C. R. Chu and F. Yang, *Biomaterials*, 2020, **228**, 119579.
48 S. Ichinose, T. Muneta, H. Koga, Y. Segawa, M. Tagami, K. Tsuji and I. Sekiya, *Lab. Invest.*, 2010, **90**, 210–221.
49 G. Pattappa, H. K. Heywood, J. D. de Bruijn and D. A. Lee, *J. Cell Physiol.*, 2011, **226**, 2562–2570.
50 A. V. Meleshina, V. V. Dudenkova, A. S. Bystrova, D. S. Kuznetsova, M. V. Shirmanova and E. V. Zagaynova, *Stem Cell Res. Ther.*, 2017, **8**, 15.
51 W. S. Toh, T. C. Lim, M. Kurisawa and M. Spector, *Biomaterials*, 2012, **33**, 3835–3845.
52 S. H. Oh, D. B. An, T. H. Kim and J. H. Lee, *Acta Biomater.*, 2016, **35**, 23–31.
53 S. Žigon-Branc, M. Markovic, J. Van Hoorick, S. Van Vlierberghe, P. Dubruel, E. Zerobin, S. Baudis and A. Ovsianikov, *Tissue Eng., Part A*, 2019, **25**, 1369–1380.
54 A. X. Sun, H. Lin, M. R. Fritch, H. Shen, P. G. Alexander, M. DeHart and R. S. Tuan, *Acta Biomater.*, 2017, **58**, 302–311.
55 T. Wang, J. H. Lai, L. H. Han, X. Tong and F. Yang, *Tissue Eng., Part A*, 2014, **20**, 2131–2139.
56 O. Chaudhuri, L. Gu, D. Klumpers, M. Darnell, S. A. Bencherif, J. C. Weaver, N. Huebsch, H.-p. Lee, E. Lippens and G. N. Duda, *Nat. Mater.*, 2016, **15**, 326–334.
57 C. Loebel, R. L. Mauck and J. A. Burdick, *Nat. Mater.*, 2019, **18**, 883–891.
58 S. Y. Wang, H. Kim, G. Kwak, H. Y. Yoon, S. D. Jo, J. E. Lee, D. Cho, I. C. Kwon and S. H. Kim, *Adv. Sci.*, 2018, **5**, 1800852.
59 B. Huang, P. Li, M. Chen, L. Peng, X. Luo, G. Tian, H. Wang, L. Wu, Q. Tian, H. Li, Y. Yang, S. Jiang, Z. Yang, K. Zha, X. Sui, S. Liu and Q. Guo, *J. Nanobiotechnol.*, 2022, **20**, 25.
60 K. Siemsen, S. Rajput, F. Rasch, F. Taheri, R. Adelung, J. Lammerding and C. Selhuber-Unkel, *Adv. Healthcare Mater.*, 2021, **10**, 2100625.